

Revised –Unmarked 2018/10/16

Antithrombin insufficiency promotes susceptibility to liver tumorigenesis

Short title: Antithrombin inhibits liver tumor

Hiroshi Iwako^{1,3)}, Hirotaka Tashiro²⁾, Sho Okimoto¹⁾, Megumi Yamaguchi^{1,3)},
Tomoyuki Abe¹⁾, Shintaro Kuroda¹⁾, Tsuyoshi Kobayashi¹⁾, Hideki Ohdan¹⁾

¹⁾Department of Gastroenterological and Transplant Surgery, Applied Life Sciences,
Institute of Biomedical & Health Sciences, Hiroshima University, Japan

²⁾Department of Surgery, Kure Medical Center and Chugoku Cancer Center, National
Hospital Organization, Japan

³⁾Department of Clinical Research, Kure Medical Center, National Hospital
Organization, Japan

Corresponding Author:

Hirotaka Tashiro, MD., PhD.

Department of Surgery, Kure Medical Center and Chugoku Cancer Center, National
Hospital Organization

3-1, Aoyama, Kure, 737-0023, Hiroshima, Japan

Tel: +81-823-22-3111, Fax: +81-823-23-8629, E-mail: htashiro@hiroshima-u.ac.jp

Author contributions: H.I. acquisition of data, analysis of data, interpretation, drafting,
revising; H.T. conception and design, drafting, interpretation, revising, approval of

submitted version; S.O. acquisition of data, analysis and interpretation; M.Y. acquisition of data and analysis; K.S. analysis and interpretation of data; T.A. acquisition of data, analysis and interpretation; T.K. analysis and interpretation of data, revising; H.O. conception and design of the study, final approval of submitted version

Declaration of Interest: The authors have no commercial associations (*e.g.*, consultancies, stock ownership, equity interest, patent/licensing arrangements) that might pose a conflict of interest related to the submitted manuscript.

Abstract

Purpose: Antithrombin (AT) is not only a major regulator of hemostasis, but it shows anti-inflammatory properties as well. We aimed to investigate whether AT-insufficient mice increases susceptibility to liver tumorigenesis.

Methods: We induced the development of liver tumor in AT-insufficient ($AT^{+/-}$) mice and *wild-type* ($AT^{+/+}$) mice, by treating them with diethylnitrosamine (DEN) and CCl_4 . The development of liver tumors and liver inflammation were compared between these mouse groups. Following this, AT was administered to the AT-insufficient mice treated with DEN and CCl_4 .

Results: Tumor size and the number of DEN and CCl_4 -induced liver tumors significantly increased in AT-insufficient mice compared with the *wild-type* mice. Serum transaminase levels, cell death, and the expression of cleaved caspase-3 in liver were increased in $AT^{+/-}$. Furthermore, hepatic neutrophil infiltrations, and serum Il-6 and Tnf- α levels were significantly elevated in AT-insufficient mice. The levels of 8-OHdG, oxidative DNA damage marker, in liver were significantly increased in AT-insufficient mice. Administration of AT led to a significant decrease in DEN and CCl_4 -induced liver injury and inflammation in AT-insufficient mice, compared with the *wild-type* group.

Conclusions: AT insufficiency led to increased susceptibility to liver tumorigenesis by increasing hepatic inflammation.

Keywords: Hepatocellular carcinoma; antithrombin; inflammation; reactive oxygen species

Introduction

Hepatocellular carcinoma (HCC) represents the third most frequent cause of cancer-related death worldwide (1). Hepatic resection is an accepted therapy for HCC, but in many patients, it is followed by HCC recurrence, with the cumulative 5-year HCC recurrence rate over 60% (2, 3). The risk factors for HCC recurrence after resection and prophylactic management of this recurrence have been extensively studied.

Inflammation-induced liver injury represents a crucial factor for the development of HCC (4). Hepatitis viruses, such as hepatitis B or hepatitis C viruses, obesity, and alcohol promote the development of HCC by inducing persistent inflammation (5). During the chronic inflammation, many intrinsic mediators of inflammation, including pro-inflammatory cytokines, eicosanoids, growth factors, and reactive oxygen species (ROS), can induce genetic and epigenetic changes, including point mutations, deletions, duplications, recombinations, and methylation of various tumor-associated genes (4, 6).

Antithrombin (AT), a heparin-binding protein and a major inhibitor of coagulation proteases, primarily thrombin and factor Xa (7), plays a central role in the regulation of hemostasis. Apart from its role in hemostasis, many studies demonstrated that AT has anti-inflammatory properties and improves the survival *in vivo*, in animal models of sepsis, ischemia-reperfusion injury, and acute organs failure (8). Furthermore, clinical trial results showed the anti-inflammatory properties of AT in patients with sepsis or disseminated intravascular coagulation (9, 10). The inhibition of nuclear factor (Nf- κ B) signaling was shown to underlie the anti-inflammatory properties of AT (11). AT

induces the release of prostacyclin from the endothelial cells, which was shown to be independent of thrombin interaction (12-14). Additionally, it directly affects leukocytes, inhibiting neutrophil migration and the adhesion to the endothelium (15).

Anti-angiogenic properties of AT have been demonstrated as well, but only of its latent and cleaved, but not native forms (16, 17). Furthermore, native AT in combination with heparin was shown to modulate tumor migration, invasiveness, and angiogenesis by inhibiting enteropeptidase (18). To date, however, AT expression has not been associated with liver tumorigenesis and tumor progression. Previously, we demonstrated that AT plasma levels represent a significant prognostic factor for overall survival and disease-free survival of patients with HCC after curative hepatectomy (19). Recently, AT has been identified as a potential putative circulating protein biomarker for HCC (20, 21).

Here, we hypothesized that AT may help prevent the development of chronic inflammation-related HCC. We examined whether AT-insufficient mice are susceptible to the development of diethylnitrosamine (DEN)-induced liver tumors.

Materials and Methods

All animal experiments were performed according to the Animal regulations of Hiroshima University. This experimental protocol was approved by the Ethics Review Committee for Animal Experimentation of the Graduate School of Biomedical Sciences at Hiroshima University (Registration number: U003490) (Hiroshima, Japan).

Mice and HCC induction

C57BL/6J mice were purchased from CLEA (Tokyo, Japan). Mice heterozygous for ATIII gene disruption, expressing approximately 50% of the normal level of AT ($AT^{+/-}$) in a C57BL/6J background were purchased from the Center for Animal Resources and Development (CARD), Kumamoto University, Japan. Male chimeric mice were mated with the *wild-type* C57BL/6J female mice. $AT^{+/-}$ pups were genotyped as previously described (22). Genomic DNA was extracted from mouse tails and used for polymerase chain reaction (PCR) analysis. The heterozygous expression of this gene ($AT^{+/-}$) does not cause embryonic lethality in mice, and the external appearance of $AT^{+/-}$ mice could not be distinguished from that of the *wild-type* mice. Homozygous deficiency of AT ($AT^{-/-}$) is lethal (22, 23). We induced HCC as previously reported, with minor modifications (24). C57BL/6J *wild-type* ($AT^{+/+}$) mice and heterozygous ($AT^{+/-}$) mice were treated using the combination of DEN (10 mg/kg, i.p.) (Wako), which was administrated at the age of 6 weeks, followed by 25 or 27 biweekly injections of carbon tetrachloride (CCl_4 , 0.5 mL/kg, i.p., dissolved in corn oil) (Wako).

Liver tumor development was evaluated by determining the number of visible tumors and measuring the size of the largest tumor after sacrifice. Livers were explanted, digitally photographed, and weighed.

Histology and immunohistological staining

For histological analysis, formalin-fixed liver tissue sections were cut, stained with hematoxylin and eosin, and examined microscopically. To assess the grade of liver fibrosis, sections were stained with Azan. Immunohistology was performed on paraffin-embedded sections using primary antibodies to cleaved caspase-3 (Cell

Signaling Technology), Ki-67 (Dako), and anti-8-hydroxyguanosine (8-OHdG) (Japan Institute for the Control of Aging). Quantification was performed using image J and Photoshop software. Cells with positive staining were counted in 10 high-power fields (HPF, $\times 200$).

Liver tumors were classified into hepatocellular adenoma (HCA), or hepatocellular carcinoma (HCC) according to modified criteria reported by Thoolen B et al (25). HCA is characterized by the presence of proliferation of benign hepatocytes without normal lobular architecture, which is sharply demarcated with compression of the adjacent normal parenchyma. HCC is characterized by the presence of trabecular or mixed growth patterns of atypical hepatocytes and sometimes accompanied by the presence of hemorrhage, necrosis, vascular and stromal invasion.

Assay for AT in mice

Blood samples were collected into 3.8% sodium citrate at a ratio of 9:1 and were centrifuged at 2000 g for 10 min to obtain plasma. AT activity was measured using N-test AT-S (Nittobo), which determines anticoagulant activity using a chromogenic substrate, according to the manufacturer's instructions.

Quantification of serum IL-6 and TNF- α

The amounts of interleukin 6 (IL-6) and tumor necrosis factor- α (TNF- α) from mice serum were quantified using enzyme-linked immunosorbent assay (ELISA) kits, according to the manufacturer's instructions (R&D Systems).

Quantification of neutrophil accumulation

Accumulation of activated neutrophil was assessed using a naphthol AS-D chloroacetate esterase kit (90C2-1KT, Sigma-Aldrich). Neutrophils within sinusoids or extravasated into the liver tissue were identified by staining and morphology, and were counted in 10 HPFs ($\times 400$).

Hepatic 8-OHdG concentration measurement

Hepatic total DNA was isolated from liver tissue by the NaI extraction technique using the DNA Extractor WB kit (Wako). The extracted DNA was prepared to reduce the variation of the enzyme reaction by using the 8-OHdG Assay Preparation Reagent Set (Wako). The hepatic 8-OHdG level was assessed using a highly sensitive ELISA kit for 8-OHdG (Japan Institute for the Control of Aging). The absorbance of the reaction products was read at 450 nm by a microreader and expressed as ng/mg DNA.

Western blot analysis

Liver segments were homogenized in lysis buffer (Cell Lysis Buffer; Cell Signaling Technology), then sonicated and pelleted. Supernatants were denatured; 50 μ g of protein was separated by way of polyacrylamide gel electrophoresis and then transferred to nitrocellulose membranes. Western blot analysis was performed using antibodies to β -actin (Abcam) and to caspase-3 (Cell Signaling Technology).

Administration of AT

For AT treatment experiments, 1500 U of human AT was dissolved in 30 mL of saline: AT (50 U/mL) was prepared. The human AT was donated by Nihon Pharmaceutic (Tokyo, Japan). AT (500 U/kg, i.p.) was intraperitoneally given to $AT^{+/-}$ mice 1 hr before DEN induction therapy, followed by 3 injection of AT per week.

Statistical analysis

Data for animals were expressed as the average (\pm SE) and statistically compared using the Student *t*-test. The tumor engraftment rates were compared by the χ^2 test. *P* values less than 0.05 were considered statistically significant. Statistical analyses were performed with SPSS software, version 16 (SPSS Japan Inc., Tokyo, Japan).

Results

AT insufficiency promotes chemically induced liver tumorigenesis

First, we determined the activity of AT in the plasma of *wild-type* ($AT^{+/+}$) and AT-insufficient ($AT^{+/-}$) mice. The mean plasma activities of AT in wild and AT-insufficient mice were 135% and 67%, respectively.

To elucidate whether AT plays a role in the inflammation-related liver tumorigenesis, we induced liver tumors by combining DEN and CCl_4 in $AT^{+/-}$ and $AT^{+/+}$ mice. These male mice were treated with DEN at the age of 6 weeks, which was followed by 25 biweekly injections of CCl_4 . Tumor incidence and tumor size were evaluated 50 weeks after DEN treatment. Liver tumors efficiently developed in $AT^{+/-}$ mice, unlike in $AT^{+/+}$ mice. Tumors with the maximum size of 12 mm developed in 5/6 ATIII-insufficient mice, but no liver tumors were observed in $AT^{+/+}$ mice (Fig. 1). Furthermore, male mice

were treated with DEN at the age of 6 weeks, followed by 27 biweekly injections of CCl₄. Tumor incidence and size were evaluated 54 weeks after the DEN treatment. Tumors developed in 5/7 *AT*^{+/+} mice, while they developed in all treated *AT*^{+/-} mice (Fig. 2A). The maximal tumor size in *AT*^{+/-} mice was shown to be significantly higher, by 4.2-fold, compared with that in the *AT*^{+/+} mice (18±5 mm versus 4.3±6 mm), as shown in Figure 2B. Tumor number was significantly increased in *AT*^{+/-} mice as well, in comparison with those in the *AT*^{+/+} mice (Fig. 2C). Histopathological analysis showed that the majority of tumors were hepatic adenoma (HAC), but HCCs were observed in some livers (Supplementary Fig. S1). Simultaneously, liver function and fibrosis were investigated. The serum levels of total bilirubin (T-Bil) were shown to be significantly higher in *AT*^{+/-} mice compared with those in the *AT*^{+/+} mice (Supplementary Fig. S2A). We detected liver fibrosis at the late stage (54 weeks) after DEN and CCl₄ by using azan staining, which showed a more developed fibrosis in *AT*^{+/-} mice than in the *AT*^{+/+} mice (Supplementary Fig. S2B). Furthermore, both untreated *AT*^{+/+} and *AT*^{+/-} mice had livers with normal appearance, without liver tumors, and showed normal liver functions (n=5) until 60 weeks after birth (Data not shown).

Increased liver injury, inflammation, and ROS production in response to DEN and CCl₄ treatment of AT-insufficient mice

Previously, it was demonstrated that the treatment of *AT*^{+/-} mice with high dose of CCl₄ (2 mL/kg body weight) leads to a more severe liver injury, compared with that in the *AT*^{+/+} mice (26). Therefore, we examined whether a low dose of CCl₄ (0.5 mL/kg body weight) following DEN can induce liver injury in *AT*^{+/-} mice. Twenty-four hours after

DEN, which was followed by two biweekly CCl₄ injections, *AT*^{+/-} mice exhibited significantly higher levels of aspartate aminotransferase (AST) and alanine aminotransferase (ALT) than the *wild-type* mice (Fig. 3A). TUNELs demonstrated hepatic apoptosis was considerably increased in *AT*^{+/-} mice following the treatment with DEN and CCl₄, compared with that in the *wild-type* mice (Fig. 3B). Additionally, hepatic levels of active caspase-3 were assessed by immunohistochemical analyses, which showed that DEN and CCl₄ can induce caspase-3 activation and that active caspase-3 level was upregulated in *AT*^{+/-} mice compared with that in the *AT*^{+/+} mice (Fig. 3C).

Furthermore, DEN treatment followed by 27 biweekly CCl₄ injections lead to a considerable increase in hepatic apoptosis in *AT*^{+/-} mice, compared with that in the *AT*^{+/+} mice (Fig. 4A). Immunohistochemical and western blot analyses showed that active caspase-3 expression was considerably upregulated in *AT*^{+/-} mice compared with that in the *AT*^{+/+} mice (Figs. 4B and 4C). Ki-67 staining showed that the DEN treatment, followed by 27 biweekly CCl₄ injections, significantly induces hepatocellular compensatory proliferation in *AT*^{+/-} mice compared with that in the *AT*^{+/+} mice (Fig. 4D).

HCC is associated with the chronic inflammation of the liver (27). Therefore, we attempted to elucidate whether DEN treatment followed by CCl₄ induces liver inflammation in *AT*^{+/-} mice. DEN treatment followed by two biweekly CCl₄ injections led to a significant increase in Il-6 and Tnf- α serum levels in *AT*^{+/-} mice, compared with those in the *wild-type* mice (Fig. 5A). Histopathological analysis, using naphthol AS-D chloroacetate esterase staining, demonstrated that DEN treatment followed by 27

biweekly CCl₄ injections led to a significant increase in chemically-induced hepatic neutrophil accumulation in *AT*^{+/-} mice compared with that in the *AT*^{+/+} mice (Fig. 5B).

ROS production may induce oxidative DNA damage, which can be detected with antibodies specific to 8-OHdG (28). Here, we assessed oxidative DNA damage caused by ROS production, using immunohistochemistry (Fig. 6A) and ELISA (Fig. 6B) with anti-8-OHdG antibodies, which showed that DEN treatment followed by two and 27 biweekly CCl₄ injection induced a significant increase in the 8-OHdG levels in the livers of *AT*^{+/-} mice, compared with those in the *wild-type* mice, respectively.

AT administration decreases liver injury and inflammation in AT-insufficient mice

We examined the activity of AT in the plasma of AT-treated mice. The mean activity of AT was shown to be 67% in *AT*^{+/-} mice before the intraperitoneal injection of AT, and it increased to 142% at day 1 after the intraperitoneal injection of AT. However, AT activity decreased to 71% at day 3 following the injection of AT (Supplementary Fig. S3). We examined whether the administration of AT suppress liver injury in *AT*^{+/-} mice. As a control, saline was intraperitoneally given to *AT*^{+/-} mice. DEN treatment followed by two biweekly CCl₄ (0.5 mL/kg body weight) injections induced a significant decrease in AST and ALT level in *AT*^{+/-} mice that received AT, compared with those in *AT*^{+/-} mice that were not treated with AT (Fig. 7A). ELISA also showed that DEN treatment followed by two biweekly CCl₄ injections induced a significant decrease in level Il-6 and Tnf- α serum levels in *AT*^{+/-} mice that received AT, compared with those in *AT*^{+/-} mice that were not treated with AT (Fig. 7B).

Discussion

In this study, we demonstrated the biological significance of endogenous plasma AT levels in modulating the development of liver tumors. To the best of our knowledge, here we demonstrated for the first time that mice with low plasma levels of AT show increased susceptibility to the development of liver tumors.

In this study, we showed that $AT^{+/-}$ mice are more susceptible to chemicals-induced liver injury. Furthermore, the administration of AT suppressed chemicals-induced liver injury in AT-insufficient mice. These results were shown to be comparable with those obtained in the previous study, which showed that $AT^{+/-}$ mice exhibit a more severe liver injury following the administration of high CCl_4 dose, in comparison with that observed in the $AT^{+/+}$ mice (26). Our results also demonstrated that hepatic apoptosis and caspase-3 expression is upregulated in the livers of $AT^{+/-}$ mice. These protective effects of the endogenous AT may be partially attributed to the anticoagulant activity of this molecule, through the inhibition of thrombin and other proteases. AT also inhibits a protease involved in the process of apoptosis, thereby diminishing the apoptotic response and increasing hepatocyte survival (26).

We demonstrated here that the neutrophil infiltration and hepatic inflammation, including the serum Il-6 and Tnf- α levels, following chemicals-induced liver injury, were increased in AT-insufficient mice, compared with those in the *wild-type* mice. Our results also showed that AT administration induced the suppression of serum Il-6 and Tnf- α levels. AT is known to have anti-inflammatory activity (8), by stimulating prostacyclin production in the endothelial cells (12). In animals, AT was shown to protect against ischemia-reperfusion injury and acute liver, lung, and kidney injuries

through the upregulation of prostacyclin expression and the inhibition of leukocyte chemotaxis and Il-6/Tnf- α expression (29-31). The results obtained here agree with those obtained in the previous reports. Anti-inflammatory activity of AT may be partially dependent on the release of PGI₂, but further studies are necessary to clarify the molecular mechanisms underlying these processes.

AT-insufficient mice show increased susceptibility to DEN and CCl₄-induced liver tumorigenesis. *AT*^{+/-} mice were shown to have increased serum Il-6 and Tnf- α levels following the chemical inducement of liver injury, and these mice exhibited increased susceptibility to the development of ROS-induced oxidative DNA damage. TNF- α , produced by the inflammatory cells in tumor microenvironment, can promote tumor cell survival through the induction of the expression of genes encoding NF- κ B-dependent anti-apoptotic molecules, and can contribute to tumor initiation by stimulating the production of genotoxic molecules, such as ROS, that can lead to DNA damage and mutations (32). IL-6 activates signal transducer and activator of transcription 3 (STAT3) inducing cell growth, cyclooxygenase-2 expression, and ROS production (32). One common ROS molecule inducing DNA damage is 8-OHdG, and the typical pattern of nucleotide alterations by 8-OHdG is G-C to T-A transversion during DNA replication, which was observed in *KRAS* and *P53* genes in liver cancers (33). Our results indicate that AT shows anti-tumor activity through the suppression of oxidative DNA damages. Therefore, the oxidative DNA damage is induced in *AT*^{+/-} mice through ROS accumulation in response to DEN and CCl₄ treatment.

Beneficial effects of AT were previously observed in patients with sepsis, suggesting that AT suppresses the inflammation (10). If the administration of AT suppresses

DEN-induced hepatocarcinogenesis in $AT^{+/-}$ mice, AT supplementation may be able to suppress HCC recurrence after hepatectomy. However, whether exogenous AT inhibits the development of ROS-induced oxidative DNA damage should be further investigated, and whether AT administration suppresses DEN-induced carcinogenesis in $AT^{+/-}$ mice.

In conclusion, AT insufficiency increases the susceptibility to liver tumorigenesis in mice through an increased inflammation.

Acknowledgments

We would like to thank Prof. Tetsuhito Kojima, Department of Medical Technology, Nagoya University School of Health Sciences (Nagoya, Japan), for the generous gift of mice heterozygous for antithrombin gene disruption, as well as Y. Ishida for the excellent technical assistance. Human AT was kindly donated by Nihon Pharmaceutic (Tokyo, Japan).

This study was partially supported by a Grant-in-Aid from the Ministry of Education, Culture, Sports, Science and Technology (15K10165), Japan and Mitsui Life Social Welfare Foundation.

References

1. Rorner A, Llovet JM, Bruix J. Hepatocellular carcinoma. *Lancet* 2012; 379: 1245-1255.
2. Fan ST, Mau Lo C, Poon RT, et al. Continuous improvement of survival outcomes of resection of hepatocellular carcinoma: a 20-year experience. *Ann Surg* 2011; 253: 745-748.
3. Portolani N, Coniglio A, Ghidoni S, et al. Early and late recurrence after liver resection for hepatocellular carcinoma: prognostic and therapeutic implications. *Ann Surg* 2006; 243: 229-235.
4. Zucman-Rossi J, Villanueva A, Nault JC, Llovet JM. Genetic landscape and biomarkers of hepatocellular carcinoma. *Gastroenterology* 2015; 149: 1226-1239.
5. El-Serag HB. Hepatocellular Carcinoma. *N Engl J Med* 2011; 365: 1118-1127.
6. Chiba T, Marusawa H, Ushijima T. Inflammation-associated cancer development in digestive organs: mechanisms and roles for genetic and epigenetic modulation. *Gastroenterology* 2012; 143: 550-563.
7. Rosenberg RD. Biochemistry of heparin antithrombin interaction, and the physiologic role of this natural anticoagulant mechanism. *Am J Med* 1989; 87: 2S-9S.
8. Wiedermann CJ, Romisch J. The anti-inflammatory actions of antithrombin-a review. *Acta Medica Austriaca* 2002; 29: 89-92.

9. Kienast J, Juers M, Wiedermann CJ, et al. Treatment effects of high-dose antithrombin without concomitant heparin in patients with severe sepsis with or without disseminated intravascular coagulation. *J Thromb Haemost* 2006; 4: 90-97.
10. Warren BL, Eid A, Singer P, et al. Caring for the critically ill patient. High-dose antithrombin III in severe sepsis: a randomized controlled trial. *JAMA* 2001; 286: 1869-1978.
11. Oelschläger C, Römisch J, Staubitz A, et al. Antithrombin III inhibits nuclear factor kB activation in human monocytes and vascular endothelial cells. *Blood* 2002; 99: 4015-4020.
12. Yamauchi T, Umeda F, Inoguchi T, Nawata H. Antithrombin III stimulates prostacyclin production by cultured aortic endothelial cells. *Biochem Biophys Res Commun* 1989; 163: 1404-1411.
13. Nakamura K, Ito T, Yoneda M, et al. Antithrombin III prevents concanavalin A-induced liver injury through inhibition of macrophage inflammatory protein-2 release and production of prostacyclin in mice. *J Hepatol* 2002; 36: 766-773.
14. Harada N, Okajima K, Kushimoto S, Isobe H, Tanaka K. Antithrombin reduces ischemia/reperfusion injury of rat liver by increasing the hepatic level of prostacyclin. *Blood* 1999; 93: 157-164.
15. Dunzendorfer S, Kaneider N, Rabensteiner A, et al. Cell-surface heparin sulfate proteoglycan-mediated regulation of human neutrophil migration by the serpin antithrombin III. *Blood* 2002; 97: 1079-1085.
16. O'Reilly MS, Pirie-Shepherd S, Lane WS, Folkman J. Antiangiogenic activity of the cleaved conformation of the serpin antithrombin. *Science* 1999; 285: 1926-1928.

17. Kisker O, Onizuka S, Banyard J, et al. Generation of multiple angiogenesis inhibitors by human pancreatic cancer. *Cancer Res* 2001; 61: 7298-7304.
18. Luengo-Gill G, Calvo MI, Martin-Villar E, et al. Antithrombin controls tumor migration, invasion and angiogenesis by inhibition of enteropeptidase. *Sci Rep* 2016; 6: 27544.
19. Iwako H, Tashiro H, Amano H, et al. Prognostic significance of antithrombin III levels for outcomes in patients with hepatocellular carcinoma after curative hepatectomy. *Ann Surg Oncol* 2012; 19: 2888-2896.
20. He X, Wang Y, Zhang W, et al. Screening differential expression of serum proteins in AFP-negative HBV-related hepatocellular carcinoma using iTRAQ-MALDI-MS/MS. *Neoplasia* 2014; 61: 17-26.
21. Awan FM, Naz A, Obaid A, et al. Identification of circulating biomarker candidates for hepatocellular carcinoma (HCC): an integrated prioritization approach. *Plos One* 2015; 10: e0138913.
22. Ishiguro K, Kojima T, Kadomatsu K, et al. Complete antithrombin deficiency in mice results in embryonic lethality. *J Clin Invest* 2000; 106: 873-878.
23. Yanada M, Kojima T, Ishiguro K, et al. Impact of antithrombin deficiency in thrombosis: lipopolysaccharide and stress-induced thrombus formation in heterozygous antithrombin-deficient mice. *Blood* 2002; 99: 2455-2458.
24. Uehara T, Ainslie GR, Kutanzi K, et al. Molecular mechanisms of fibrosis-associated promotion of liver carcinogenesis. *Toxicol Sci* 2013; 132: 53-63.

25. Thoolen B, tenkate FJW, van Diest PJ, et al. Comparative histomorphological review of rat and human hepatocellular proliferative lesions. *J Toxicol Pathol* 2012; 25: 189-199.
26. Guerrero JA, Teruel R, Martinez C, et al. Protective role of antithrombin in mouse models of liver injury. *J Hepatol* 2012; 57: 980-986.
27. Maeda S, Kamata H, Luo JL, Leffert H, Karin M. Ikk β couples hepatocyte death to cytokine-driven compensatory proliferation that promotes chemical hepatocarcinogenesis. *Cell* 2005; 121: 977-990.
28. Shibutani S, Takeshita M, Grollman AP. Insertion of specific bases during DNA synthesis past the oxidation-damaged base 8-oxdG. *Nature* 1991; 349: 431-434.
29. Wang J, Wang Y, Wang J, et al. Antithrombin is protective against myocardial ischemia and reperfusion injury. *J Thromb Haemost* 2013; 11: 1020-1028.
30. Rehberg S, Yamamoto Y, Sousse L, et al. Antithrombin attenuates vascular leakage via inhibiting neutrophil activation in acute lung injury. *Crit Care Med* 2013; 41: e439-e446.
31. Wang F, Zhang G, Lu Z, et al. Antithrombin III/serpinC1 insufficiency exacerbates renal ischemia/reperfusion injury. *Kidney Int* 2015; 88: 796-803.
32. Lin WW, Karin M. A cytokine-mediated link between innate immunity, inflammation, and cancer. *J Clin Invest* 2007; 117: 1175-1183.
33. Nakae D, Kobayashi Y, Akai H, et al. Involvement of 8-hydroxyguanine formation in the initiation of rat liver carcinogenesis by low dose levels of N-nitrosodiethylamine. *Cancer Res* 1997; 57: 1281-1287.

Figure Legends

Fig. 1. AT insufficiency promotes DEN and CCl₄-induced liver tumorigenesis. WT (n=6) and AT-insufficient (n=6) mice were treated with a combination of DEN (10 mg/kg) and 25 biweekly injections of CCl₄ (0.5 mL/kg). DEN- and CCl₄-induced liver tumors are presented here. The incidence of tumorigenesis was compared using the χ^2 . **P*<0.05.

Fig. 2. AT-insufficiency promotes DEN and CCl₄-induced liver tumorigenesis. WT (n=7) and AT-insufficient (n=8) mice were treated with a combination of DEN treatment (10 mg/kg) and 27 biweekly injections of CCl₄ (0.5 mL/kg). (A) DEN- and CCl₄-induced liver tumors at 60 weeks. (B) Maximal tumor size in WT and AT-insufficient mice. (C) Average number of liver tumors in WT and AT-insufficient mice. Results are presented as mean±SE. Student's t-test used: **P*<0.05.

Fig. 3. AT-insufficiency exacerbates liver injury, hepatocellular apoptosis, and inflammation after short-course DEN and CCl₄ treatment. WT and AT-insufficient mice were treated with DEN (10 mg/kg) and two biweekly injections of CCl₄ (0.5 mL/kg). (A) Serum ALT and AST level were assessed. (B) TUNEL assay results (Scale bar, 100 μ m). The apoptotic index was determined by counting TUNEL-positive cells. (C) Cleaved caspase-3 staining (Scale bar, 100 μ m), and cleaved caspase-3 index. The obtained results are presented as mean±SE. (n=6 in each group). Student's t-test used: **P*<0.05.

Fig. 4. AT-insufficiency exacerbates liver injury, and induces hepatocellular apoptosis and proliferation after long-term DEN and CCl₄ treatment.

WT (n=7) and AT-insufficient (n=8) mice were treated with DEN (10 mg/kg), followed by 27 biweekly injections of CCl₄ (0.5 mL/kg). (A) TUNEL assay results (Scale bar, 100 μ m). The apoptotic index was determined by counting TUNEL-positive cells. (B) Cleaved caspase-3 staining (Scale bar, 100 μ m), and the cleaved caspase-3 index. (C) Cleaved caspase-3 expression levels were determined by western blotting. (D) Ki-67 staining (Scale bar, 100 μ m), and Ki-67 index determination. Results are presented as mean \pm SE (n=6 in each group). Student's t-test was used: * P <0.05.

Fig. 5. AT-insufficiency exacerbates DEN and CCl₄-induced inflammation. (A) WT and AT-insufficient mice were treated with a combination of DEN (10 mg/kg), followed by two biweekly injections of CCl₄ (0.5 mL/kg). Serum Il-6 and Tnf- α levels were determined by ELISA. (B) WT and AT-insufficient mice were treated with a combination of DEN (10 mg/kg), followed by 27 biweekly injections of CCl₄ (0.5 mL/kg). Neutrophil infiltration in liver was assessed by naphthol AS-D chloroacetate esterase staining. Neutrophils were counted in 10 HPF. Results are presented as mean \pm SE (n=6 in each group). Student's t-test used: * P <0.05.

Fig. 6. AT-insufficiency promotes DEN and CCl₄-induced oxidative DNA damage in liver. (A) WT and AT-insufficient mice were treated with a combination of DEN (10 mg/kg), followed by two biweekly injections of CCl₄ (0.5 mL/kg). Liver sections were

stained with anti-8-OHdG antibodies (Scale bar, 100 μ m). (B) WT and AT-insufficient mice were treated with a combination of DEN (10 mg/kg), followed by 27 biweekly injections of CCl₄ (0.5 mL/kg). Hepatic 8-OHdG levels were measured by ELISA.

Results are presented as mean \pm SE (n=6 in each group). Student's t-test used: * P <0.05.

Fig. 7. AT administration suppresses DEN and CCl₄-induced hepatic injury and inflammation in AT-insufficient mice. AT-insufficient (n=10) mice were treated with DEN (10 mg/kg), followed by two biweekly injections of CCl₄ (0.5 mL/kg). Five mice were treated with human AT (500 U/kg, i.p.), while five other mice were treated with saline. AT was intraperitoneally given 1 hr before DEN induction therapy, followed by 3 injections of AT per week for 2 weeks. (A) Serum ALT and AST level were assessed. (B) Serum Il-6 and Tnf- α levels were determined by ELISA. The results are presented as mean \pm SE. Student's t-test used: * P <0.05.

Supplementary Fig. S1. Histopathological findings of DEN and CCl₄-induced liver tumorigenesis. (A) Representative hematoxylin and eosin-stained images of liver adenoma (scale bar, 100 μ m). (B) Representative hematoxylin and eosin-stained images of hepatocellular carcinoma (scale bar, 100 μ m).

Supplementary Fig. S2. AT insufficiency exacerbated DEN and CCl₄-induced liver dysfunction and hepatic fibrosis. Wildtype (n=7) and AT-insufficient (n=8) mice were treated with a combination of DEN (10 mg/kg) given at the age of 6 weeks, followed by 27 biweekly injections of CCl₄ (0.5 mL/kg). (A) Serum T-Bil levels were assessed. (B) Representative Azan-stained images of liver tissues (scale bar, 100 μ m). Liver fibrotic areas were measured. Values are expressed as the mean \pm SE. The Student t-test was used for analysis. * $p < 0.05$.

Supplementary Fig. S3. Kinetics of plasma AT in AT-insufficient (*AT*^{+/-}) mice after intraabdominal injection of AT. Plasma activities of AT in each group (n=3) were measured before, 24 hr, and 72 hr after intraabdominal injection of AT (500IU/kg). Values are expressed as the mean \pm SE. The Student t-test used for analysis. * $p < 0.05$.

Fig.3.

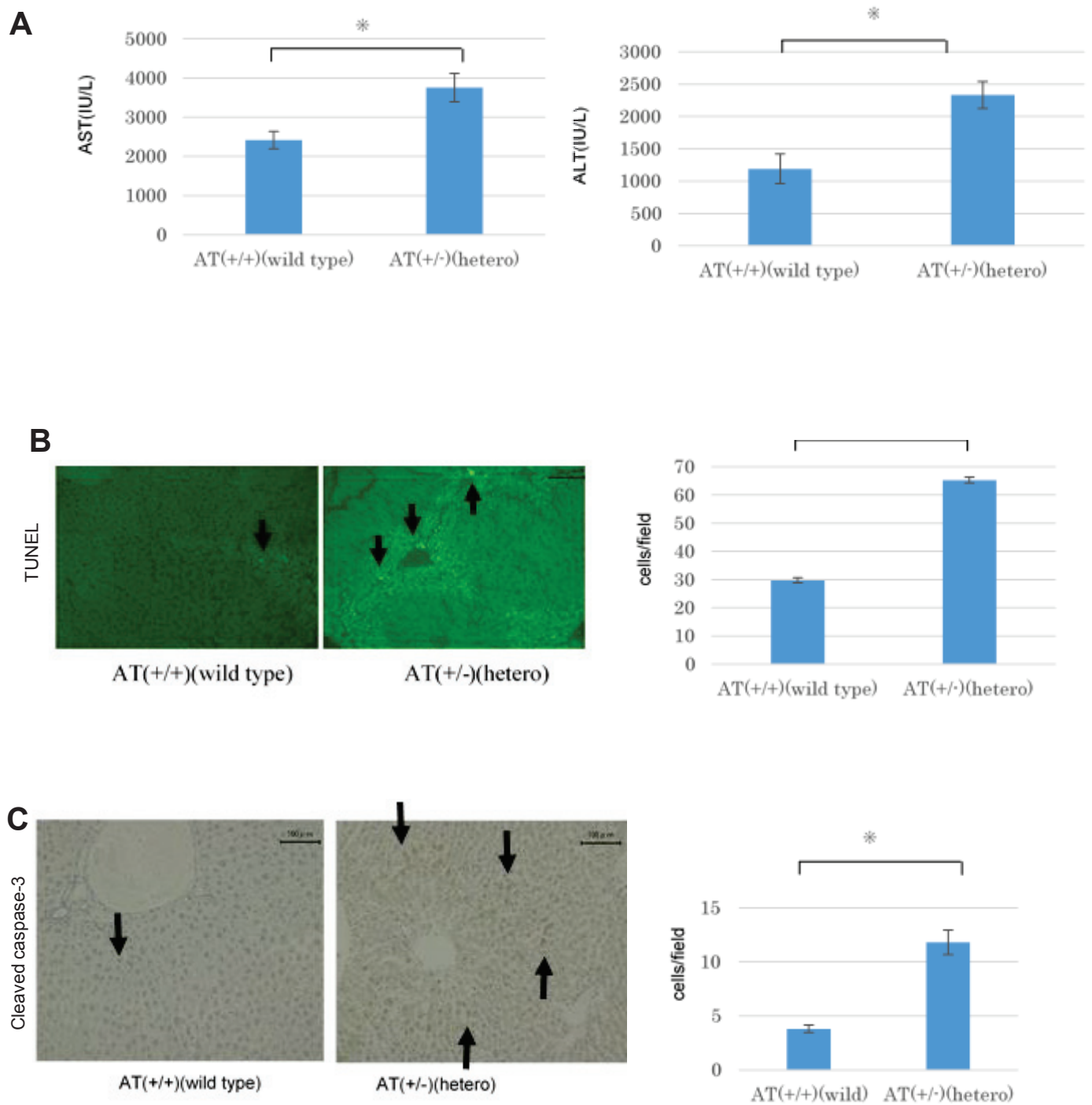


Fig.4.

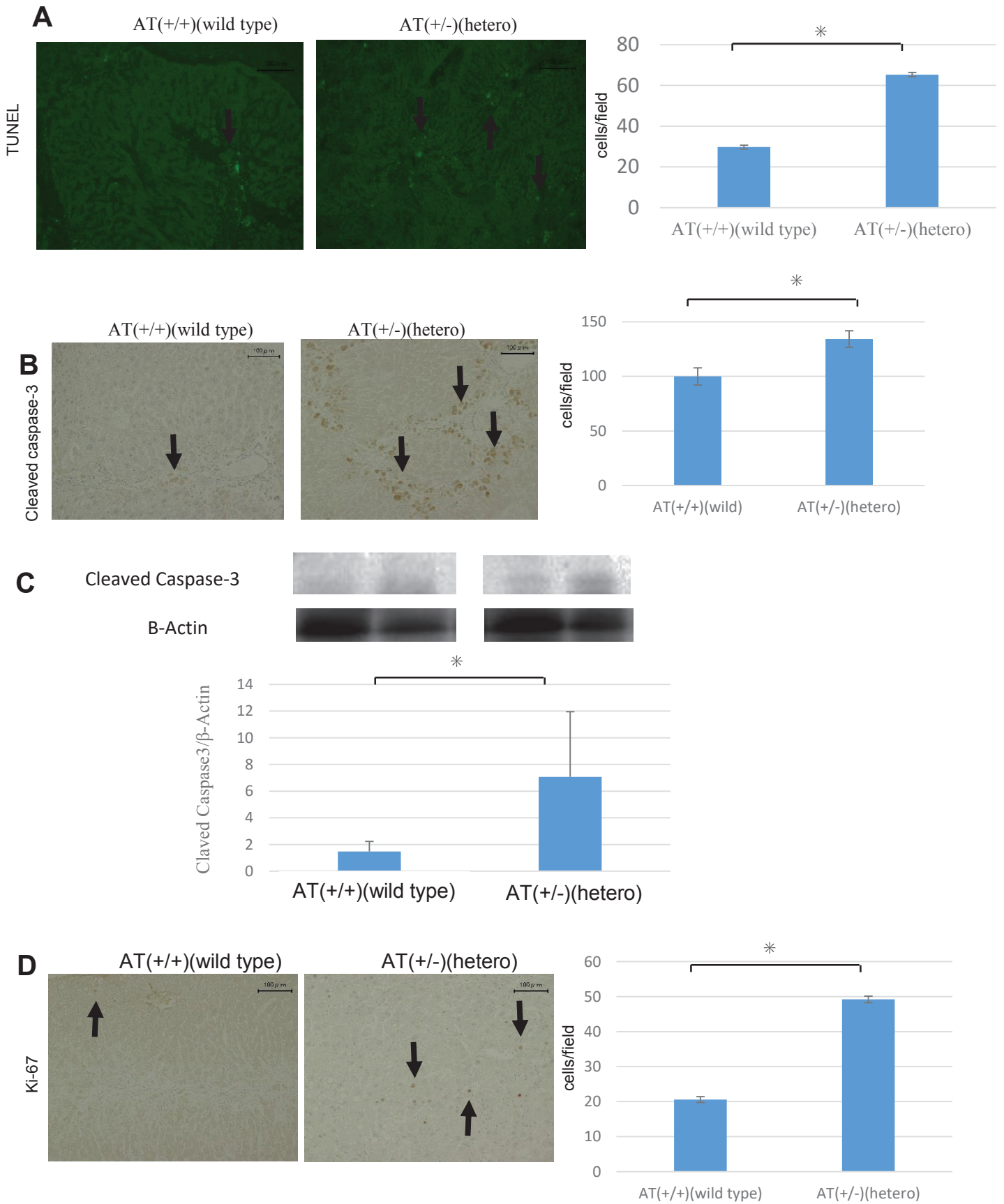
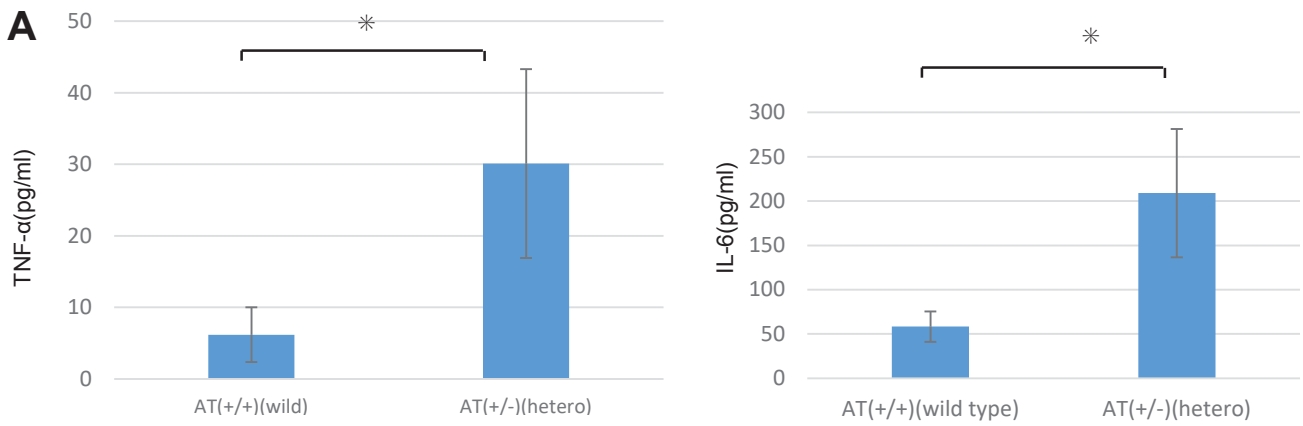


Fig.5.



B naphthol AS-D chloroacetate esterase staining

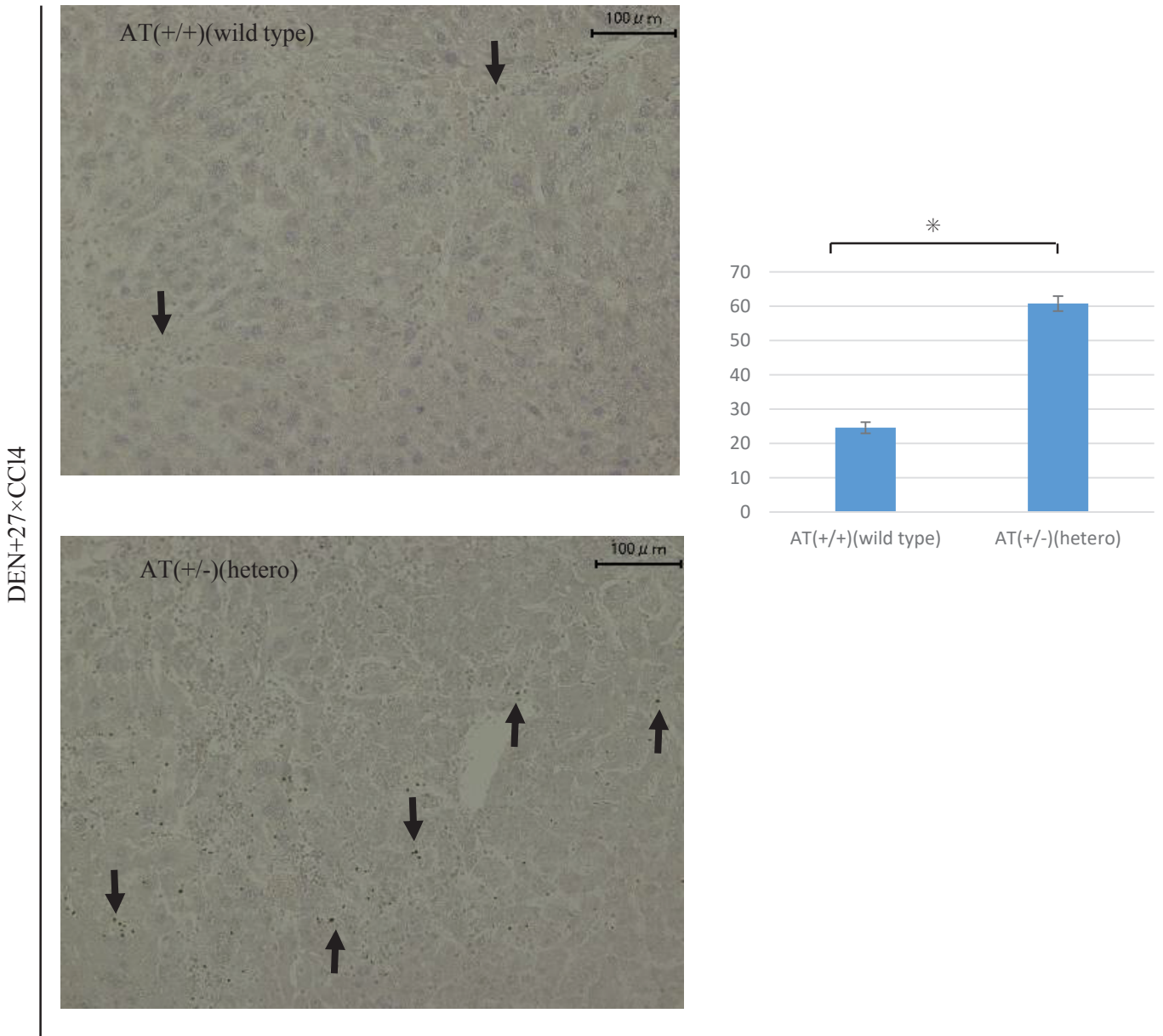
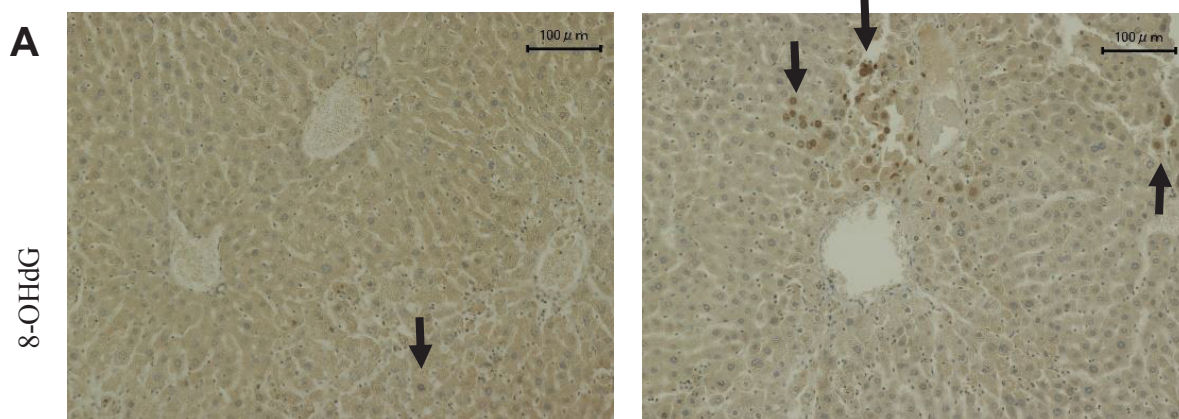


Fig.6.



AT(+/+)(wild type)

AT(+/-)(hetero)

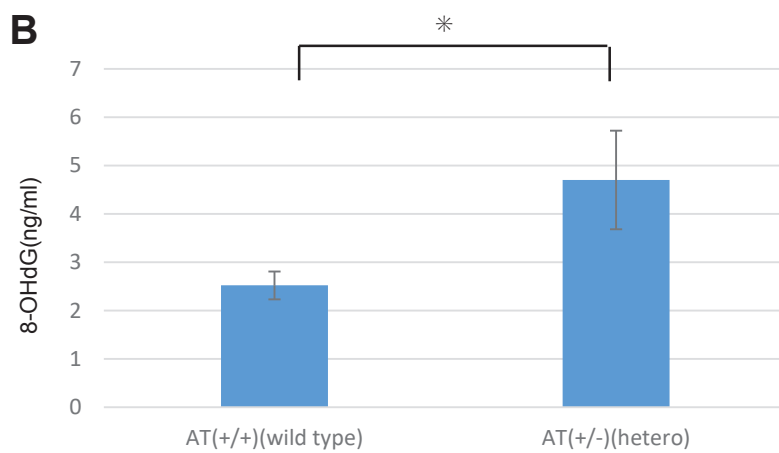
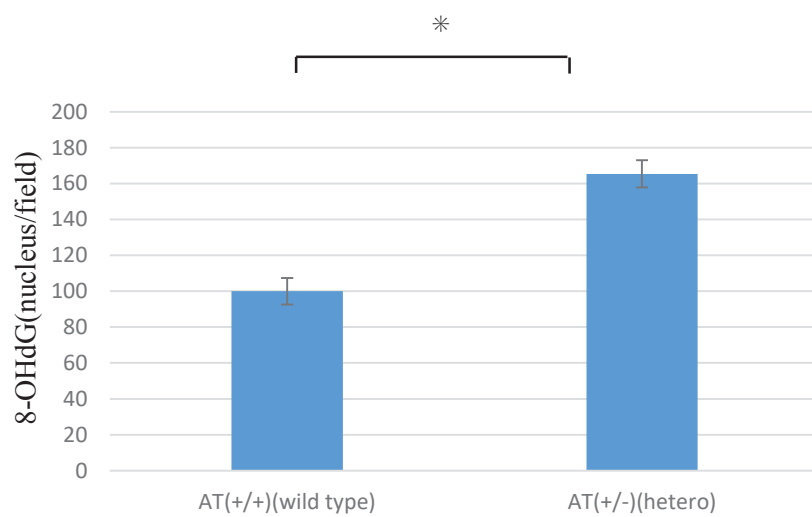
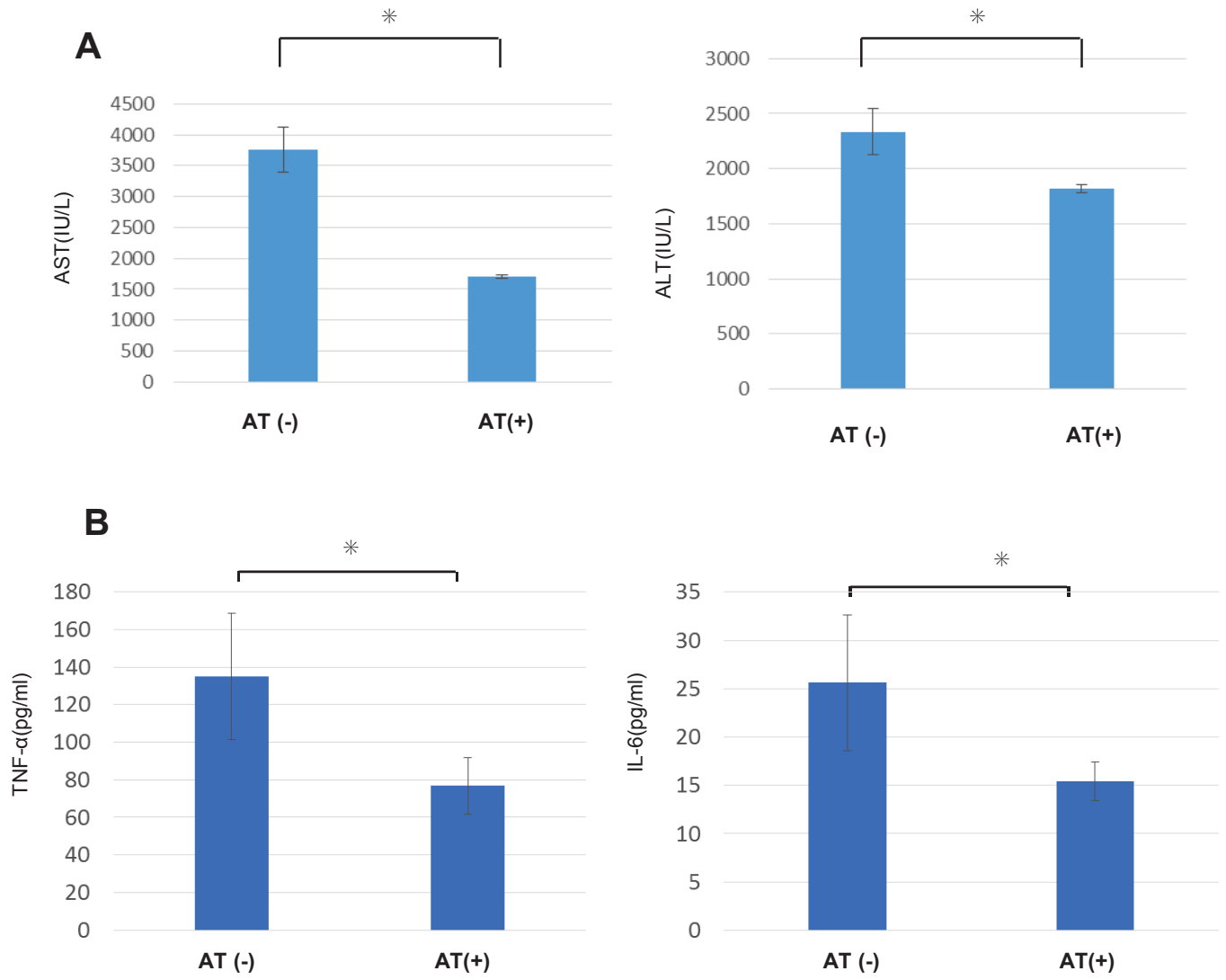
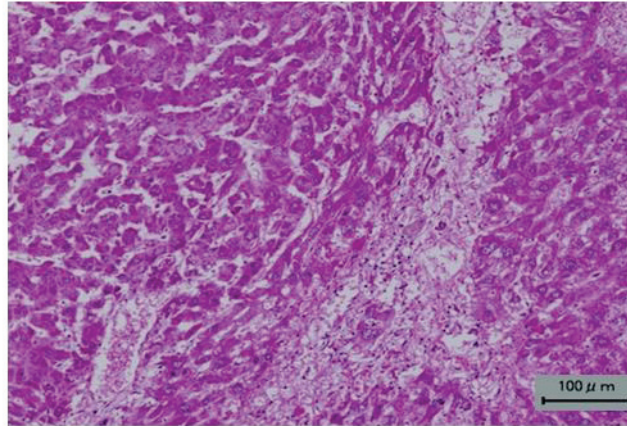


Fig.7.

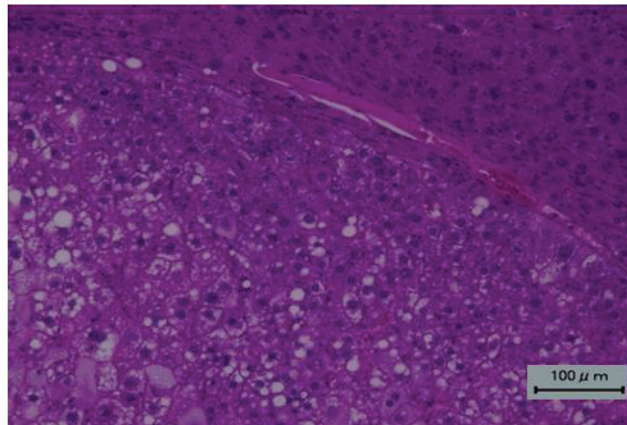


Supplementary Fig. S1

A.



B.

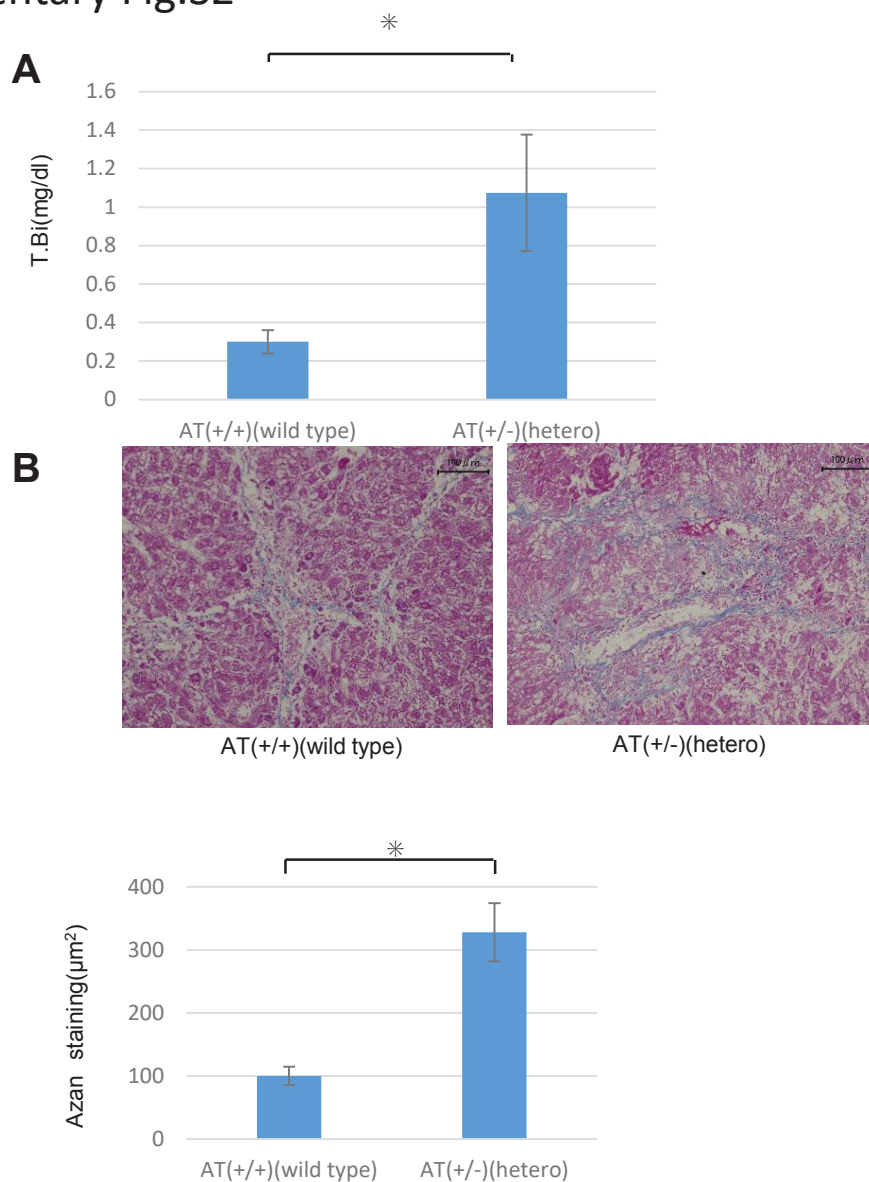


Supplementary Fig. S2. Histopathological findings of DEN and CCl₄-induced liver tumorigenesis. (A)

Representative hematoxylin and eosin-stained images of liver adenoma (scale bar, 100 μm). (B)

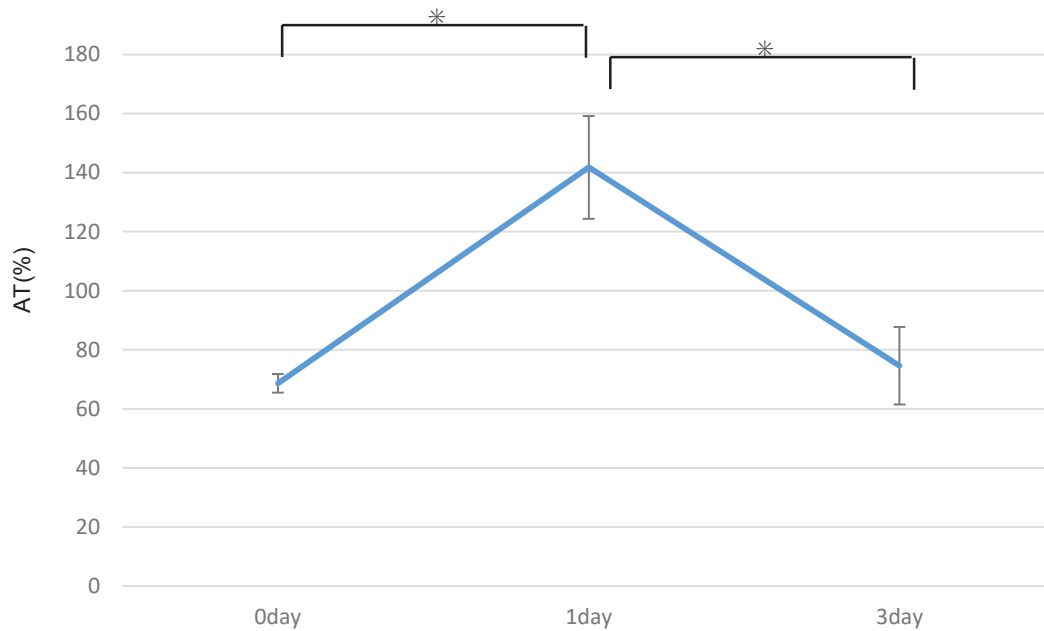
Representative hematoxylin and eosin-stained images of hepatocellular carcinoma (scale bar, 100 μm).

Supplementary Fig.S2



Supplementary Fig. S3. AT insufficiency exacerbated DEN and CCl₄-induced liver dysfunction and hepatic fibrosis. Wildtype (n=7) and AT-insufficient (n=8) mice were treated with a combination of DEN (10 mg/kg) given at the age of 6 weeks, followed by 27 biweekly injections of CCl₄ (0.5 mL/kg). (A) Serum T-Bil levels were assessed. (B) Representative Azan-stained images of liver tissues (scale bar, 100 µm). Liver fibrotic areas were measured. Values are expressed as the mean ± SE. The Student t-test was used for analysis. **p* < 0.05.

Supplementary Fig. S3



Supplementary Fig. S4. Kinetics of plasma AT in AT-insufficient ($AT^{+/-}$) mice after intraabdominal injection of AT. Plasma activities of AT in each group (n=3) were measured before, 24 hr, and 72 hr after intraabdominal injection of AT (500IU/kg). Values are expressed as the mean \pm SE. The Student t-test used for analysis. * $p < 0.05$.